Phase change-driven photoacoustic oscillations induced by periodic irradiation

Nathan Blanc ; Guy Z. Ramon

Check for updates

CrossMark

View Online

Export Citation

Applied Physics Letters

AIP Publishing

Phase change-driven photoacoustic oscillations induced by periodic irradiation

Nathan Blanc[1,2] (iD) and Guy Z. Ramon[1,2,a] (iD)

AFFILIATIONS

[1]Grand Technion Energy Program (GTEP), Technion - Israel Institute of Technology, Haifa 32000, Israel
[2]Department of Civil & Environmental Engineering, Technion - Israel Institute of Technology, Haifa 32000, Israel

[a]Author to whom correspondence should be addressed: ramong@technion.ac.il

ABSTRACT

The photo-acoustic effect is a well-documented phenomenon in which the periodic irradiation of an absorbing media produces an acoustic wave, modulated by thermal expansion. However, little is known about the effect imparted by phase change on this mode of energy conversion, nor has it been considered as a potential method of power production. Herein, we report high-amplitude photo-acoustic oscillations, of up to 145 dB, induced upon irradiation of a water film on the wall of an acoustic loop resonator. While the driving power is quite low (~4 W), the photo-acoustic oscillations are shown to be significantly amplified by the introduction of phase change in the acoustic cycle. A reduced-order model is formulated and is able to recover key characteristics of the acoustic oscillations, in reasonable agreement with experimental results, and confirms the underlying mechanism of pressure modulation by the phase change. The results presented here can potentially pave the way to improved, solar-driven acoustic energy conversion devices.

Thermoacoustic phenomena are the result of interactions between oscillating pressure, velocity, and temperature fields in acoustic waves. These interactions lead to energy conversion between heat fluxes and acoustic power. Thermoacoustic engines and heat pumps (converting heat to acoustic power and vice versa, respectively) have been utilized in various applications, ranging from electricity generators for developing communities,[1] through natural gas liquefaction[2] and waste heat recovery[3] to space applications.[4,5] Thermoacoustic conversion of heat to acoustic power relies on the proper phasing of the oscillating temperature and pressure fields, which can lead to the amplification of perturbations in the fluid. In "traditional" thermoacoustic engines, this instability—converting heat into sound—is triggered by establishing spatial gradients in the mean temperature profile.[6]

The conversion of heat to sound can also occur during periodic irradiation of an absorbing media. This is known as the photo-acoustic effect, first documented by Bell[7] and since extensively researched in the context of biomedical imaging[8] and spectroscopy.[9] Furthermore, the impact of phase change on the photo-acoustic effect has been discussed in the literature,[10,11] where it was theoretically predicted that evaporation and condensation will alter a photoacoustic signal, potentially leading to inaccurate measurements. Arnott et al.,[12]

investigated the photoacoustic signal from volatile aerosols. However, no experimental quantification of phase change effects, relative to the dry base state, has been reported in the literature, and the context of energy conversion was not considered. Meanwhile, the introduction of phase change to the acoustic cycle in thermoacoustic systems has been shown to improve performance substantially, leading to increased pressure amplitudes at lower heat input and temperatures.[13–19]

Motivated by the prospect of photo-excited thermoacoustic engines, we present experimental evidence of this operational mode, demonstrating the generation of high-amplitude photo-acoustic oscillations, driven by periodic irradiation of a looped resonator. In particular, we show that these oscillations are significantly enhanced by the feedback provided via evaporation and condensation at the resonator wall.

The experimental system is presented in Fig. 1(a) and consists of an 8-Watt CO_2 laser (MERIT-S, by Access Lasers), directed into a looped-tube resonator filled with atmospheric air (A discussion on air properties and the effect of ambient conditions can be found in the supplementary material). The resonator consists of a 16 mm-diameter, 0.67 m-long aluminum tube, connected through conic sections to a 21 mm-diameter, 2 m-long steel tube. The laser beam enters the resonator through an 8 mm-diameter hole in one side of the aluminum
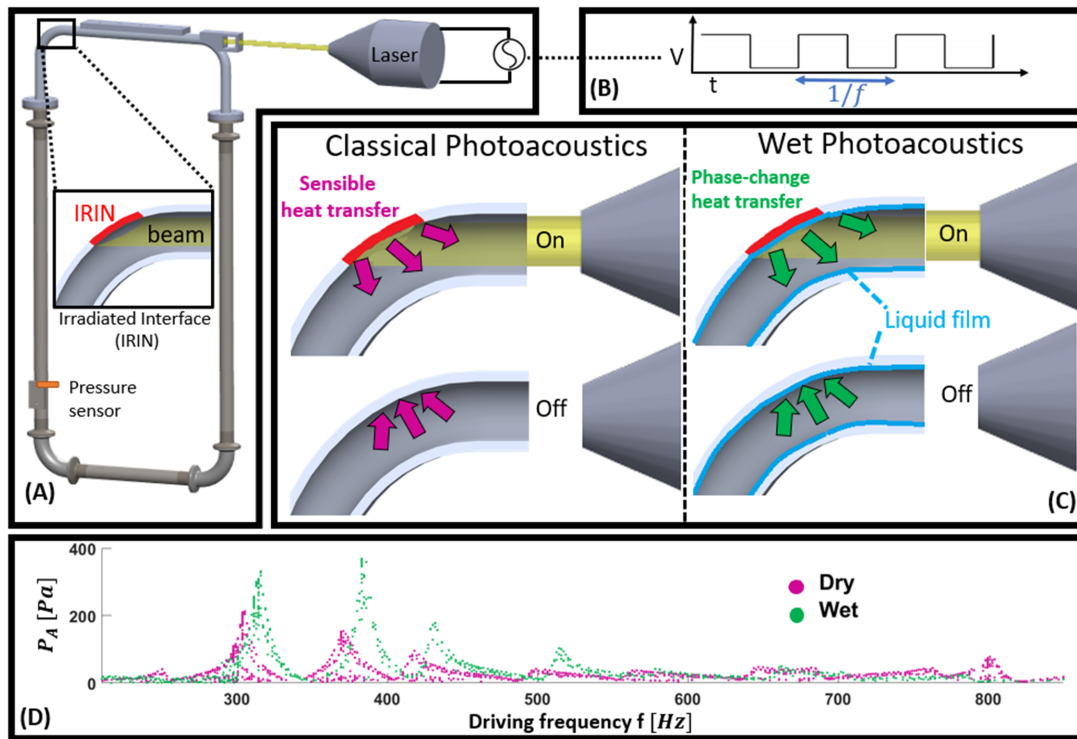
FIG. 1. (a) Schematic of the experimental apparatus: an 8 W CO_2 laser is directed at a looped resonator, periodically turned on and off by an electric signal (b). This leads to periodic irradiation of the inner resonator wall at the irradiated interface (IRIN). High-amplitude photo-acoustic waves are created in the resonator, at the driving frequency of the laser. (c) Schematic of the conversion mechanism, for both dry and wet cases: when the laser is turned on and off, heat is transferred from the IRIN to the fluid and back, respectively, driving an acoustic wave. When the resonator wall is wet, evaporation and condensation are added to the acoustic cycle, resulting in latent heat transfer, which enhances the photo-acoustic conversion. (d) The measured peak amplitude of the generated acoustic field within the resonator, as a function of the driving frequency sweep applied to the laser. The "wet" mode results in a higher pressure amplitude.

section and hits the opposing end [see illustration in Fig. 1(a)]. A picture of the actual experimental system is available in the supplementary material. Periodic irradiation was achieved by driving the laser with a square-wave input source at different frequencies, as illustrated in Fig. 1(b). In some experiments, labeled "wet," the interior surface of the resonator was pre-wetted with water by passing a soaked rag through the aluminum section three times, creating a liquid film on the surface. The envisioned mechanism, which draws inspiration from some of our previous work,[16,20] is illustrated schematically in Fig. 1(c)—the laser beam is turned on and off periodically, generating the concurrent pulsed heating of the irradiated resonator section. Consequently, heat is transferred to and from the irradiated section to the adjacent fluid, due to phase-lags generated by the transient response to the pulsed heating. Notably, in the presence of the liquid film, the periodic heat transfer is augmented by evaporation and condensation. The added mass transfer creates an additional mode of pressure-volume response and, hence, mechanical work.[16,17] Our main aim with the performed experiments was to examine the response of the system, in terms of the acoustic pressure, to the temporal excitation and, particularly, assess the magnitude of enhancement created by the phase change.

The temporal pressure variations were measured using a pressure sensor (Endevco MEGGITT 8530), placed 1.2 m away from the location of the hole in the resonator [see Fig. 1(a)]. The pressure amplitude was obtained by fitting a Fourier series to the pressure signal and retrieving the absolute value of the maximal term in the series. We note that this method only accounts for the most prominent acoustic frequency in the acoustic signal. This response frequency was found equal to the driving frequency of the laser, with deviations <1%. Results from a representative set of experiments are shown in Fig. 1(d), demonstrating the generation of large amplitude pressure oscillations and a significant enhancement due to the phase change—more than a factor of 2. We note that amplification of a photo-acoustic signal due to phase change is in contrast to previous reports, which mainly demonstrated attenuation.[10,11] We believe that the presence of sharp temperature gradients in our configuration, relative to the small gradients in aerosol suspensions addressed in previous work. We believe that the presence of sharp temperature gradients in our configuration, relative to the small gradients in aerosol suspensions addressed in previous work, is the reason for this difference. The amplification of sound due to thermal interactions typically requires working above a critical temperature gradient. We believe that the same is true for the mechanism described here. In order to gain further insight into the mechanism and the experimental measurements, a simplified, reduced-order model was formulated, accounting for

radiative heating, conduction in the solid and the fluid dynamics (see schematic representation of the model in Fig. 2).

We note that 2D or 3D modeling of the flow field and heat transfer in the resonator would certainly make the model more accurate. However, such models are highly non-trivial—thermoacoustic effects are often not accurately captured with traditional CFD tools due to numerical dissipation,[6] and further coupling with the heat transfer in the resonator wall would likely prove even more complicated. Since the experiments are the focal point of the present study, the utility of the model is complementary and aimed primarily at establishing the mechanism at play. Hence, The acoustic field is modeled using a 1D "lumped" approach, which has been used extensively for thermoacoustic energy conversion, with impressive accuracy.[21,22] The irradiation on the surface and the heat transfer inside the solid are treated with a 0-order model.

In our model, the irradiated region of the resonator wall is considered to be circular, with a diameter identical to that of the laser beam D_{beam}. This circular region, in turn, is in thermal contact with a semi-infinite solid on one side and a fluid on the other. Heat transfer in the solid is treated as that in an infinite domain, due to the high heat capacity of the metal relative to the low heat input from the laser.[23] The radiated heat transferred from the laser to the solid was assumed to oscillate sinusoidally,

$$Q_{rad}(t) = Q_0(1 + \sin(\omega t)), \qquad (1)$$

where $Q_0 = 4W$ is half of the rated laser power and $\omega = 2\pi f$ is the angular frequency. The heat transfer to the solid was estimated as[23]

$$Q_s = Sk_s(T_s - T_{out}), \qquad (2)$$

where $S = 2D_{beam}$ is the shape factor, k_S is the thermal conductivity, T_s is the solid temperature of the solid, and $T_{out} = 300K$ is the room

temperature. The heat transfer between the solid and fluid is assumed to follow

$$Q_{sf} = \psi(T_s - T_f) + \dot{m}l_h, \qquad (3)$$

where ψ is the heat transfer coefficient (discussed in the next paragraph), l_h is the latent heat of evaporation, and $\dot{m}$ is the mass flux generated through evaporation and condensation, which, based on the Clausius–Clapeyron equation and a heat/mass transfer analogy, can be expressed as

$$\dot{m} = \begin{cases} 0 & dry \\ \dfrac{\psi}{c_p Le}\left(e^{\frac{l_h(\gamma-1)(T_b-T_s)}{c_p\gamma T_b T_s}} - e^{\frac{l_h(\gamma-1)(T_b-T_f)}{c_p\gamma T_b T_f}}\right) & wet \end{cases}, \qquad (4)$$

where c_p is the heat capacity of the fluid, $Le = \alpha/D$ is the Lewis number, T_b is the boiling point, γ is the specific heat ratio, and T_f is the fluid temperature. We note that Eq. (4) is based on the assumption of fast kinetics (diffusion-limited regime), which is very common in problems involving flow and evaporation/condensation.[23]

The above set of equations was solved, along with the transient, 1D compressible continuity, momentum, and energy equations, where

$$\frac{Q_{sf}}{\pi r^2 D_{beam}} \qquad (5)$$

is a source term in the energy equation. We note that an appropriate value of Ψ proved difficult to obtain from the literature, since existing heat transfer correlations for oscillating flow are valid for much larger displacement fields[24,25] or much smaller tube dimensions.[26,27] Furthermore, these account for the time-averaged heat transfer in a
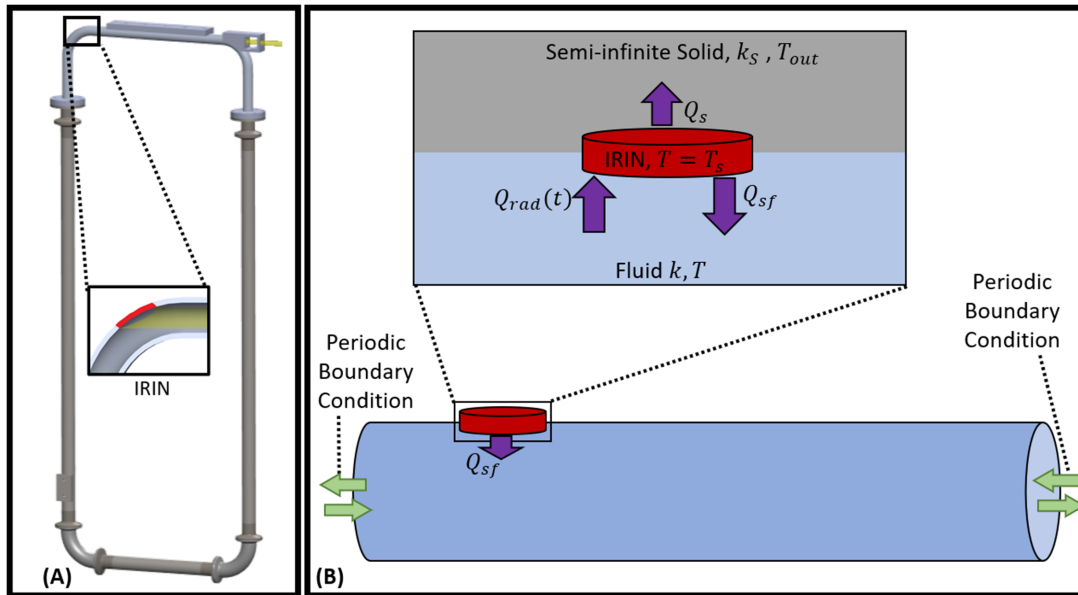
FIG. 2. Reduced order model (b) of the system (a). The model consists of a 1D model for the flow and a 0D model for the irradiated interface (IRIN) accounting for solid conduction, radiation, and fluid–solid heat transfer. Periodic boundary conditions are imposed on the flow.

purely parallel flow, where heat transfer is by conduction through the boundary layer. In our system, the velocity field is also expected to possess a radial component, driving air toward and away from the irradiated section of the resonator wall. The magnitude of the heat transfer due to these oscillations is difficult to evaluate, but it can be expected to be proportional to both the acoustic displacement $\zeta = v_1/\omega$ and to the thermal penetration depth $\delta_\alpha = \sqrt{\alpha/2\omega}$, where v_1 is the acoustic velocity amplitude in the radial direction and α is the thermal diffusivity. Therefore, we use $\psi = c_1\omega^{-3/2}$, where c_1 is a constant determined from the experimental results. The rationale for this power law is further explained in the supplementary material. The equations are solved using an upwind, Crank–Nicholson method with periodic boundary conditions at both ends of the domain. Time integration continued until a limit cycle was reached, and the amplitude was defined as the difference between minimal and maximal pressure within the cycle.

Results obtained from the numerical calculations for the pressure amplitude at the three most prominent acoustic frequencies (the first three resonant modes) are presented in Fig. 3, alongside the experimentally measured values. The experimental measurements are essential values, and frequencies of the first three peaks are shown in Fig. 1(d). Experimental results indicate a pressure amplitude of up to 180 Pa (139 dB) for the dry mode and up to 380 Pa (145 dB) for the wet mode. Because the acoustic power is, generally speaking, proportional to the pressure amplitude squared, this indicates that the introduction of phase change in the acoustic cycle can more than double the conversion efficiency and the generated acoustic power. An interesting feature in both numerical and experimental results is the relatively high intensity of the harmonics compared to the fundamental frequency. In the wet mode, the highest amplitude is not at the fundamental frequency, but, rather, at the first harmonic. This counter-intuitive result could be explained by the positive dependence of thermoacoustic conversion efficiency on frequency (see, for example, Ref. 28). This improved efficiency is, in turn, countered by viscous and thermal relaxation losses that increase at higher frequencies as well as the inverse relation between ψ and ω. The trade-off between these effects leads to an optimal working frequency that is not necessarily the fundamental frequency.

In general, the main effects discussed previously and observed experimentally are reasonably captured by the model. However, as already noted, while the theory predicts "resonant" frequencies ($f_n = na/L$ or $\omega_n = 2\pi na/L$, where n is an integer or half-integer and a is the speed of sound), the actual resonant frequencies deviated substantially from these values. This is likely due to the more complex acoustic field generated in the non-ideal resonator used in the experiments. The hole, through which the laser entered the resonator, is known to have a significant influence on both the resonant modes and their corresponding sound pressure levels.[29] Indeed, reduction in the acoustic impedance due to the hole is expected to result in intermediate harmonics, between half and full wavelength, as occurred in our experiments.[29] In the dry case, and the wet case at the lower frequencies, the deviation of the pressure amplitude between experiment and theory is between 15% and 30%. This deviation is similar to reported thermoacoustic literature, both dry[30,31] and wet.[16,19,32] However, at higher frequencies, the deviation of the wet case is more than 100%. Furthermore, at very high frequencies, the wet case exhibits lower pressure amplitudes than the dry case, in contrast to the expected behavior, which was demonstrated at low frequencies. We note that humidity cannot account for this difference [a discussion on the effect
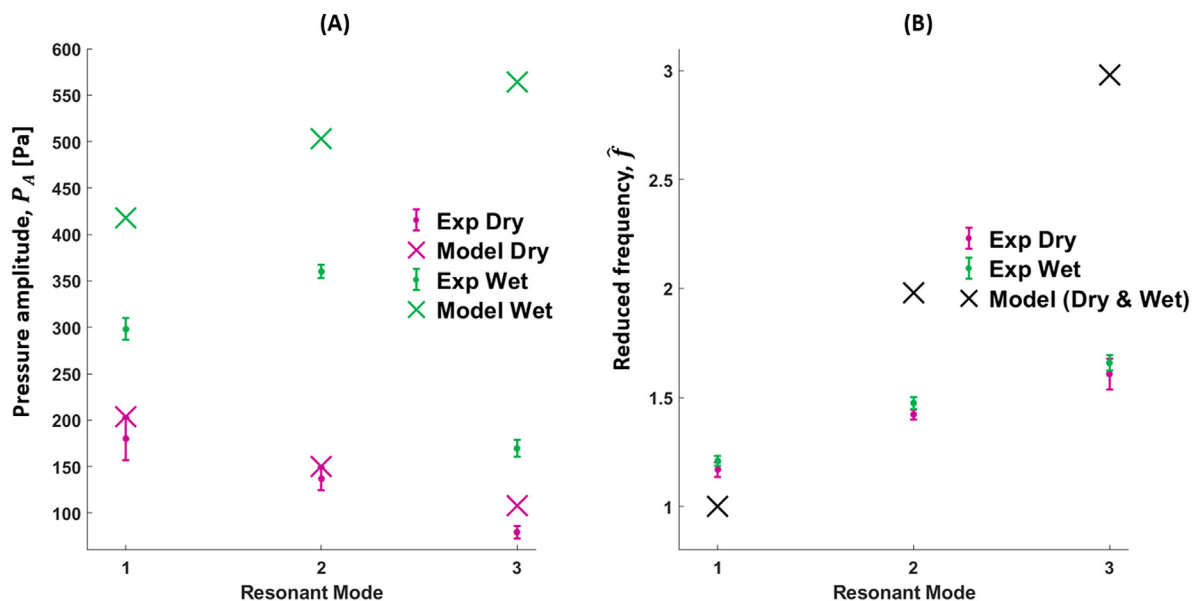
FIG. 3. Experimental measurements and model calculations, for the dry and wet systems. (a) The Pressure amplitude, shown for the first 3 resonant modes of the system, highlighting the enhancement in the "wet" system, in which the maximal pressure amplitude was more than twofold larger than the dry case. (b) The corresponding reduced frequency, $\hat{f} = f/(a/2L)$ (scaled by the natural frequency of the resonator), exhibits a significant deviation between model and experiments. While the model captures several key characteristics of the experiment, the deviation is most notable in the behavior of the wet mode at high frequencies and the system resonant frequencies.

of humidity can be found in the supplementary material]. However, it may be attributed to time-averaged mass dispersion, ("streaming") not accounted by the linear model presented here. Several forms of streaming are known to occur in thermoacoustic devices, especially near bends and near the thermoacoustic conversion core.[6] The existence of an orifice can also drive Eckert streaming,[33] which is known to be quadratically proportional to the frequency.[34] Due to the latent heat carried by the streaming flow, the enthalpy flux in the wet case is much larger than in a dry case. As an illustration, if the streaming flow is over a temperature difference of $5\,°C$, between $35\,°C$ near the irradiated interface and $30\,°C$ in the rest of the resonator. The amount of heat carried by this flow in the dry case will be equal to $\dot{H}_{dry} = \dot{V}\rho c_p \Delta T$, where $\dot{H}$ is the enthalpy flux and $\dot{V}$ is the time-averaged volumetric flow rate. However, in the wet case there will be an additional flow of latent heat due to the difference in water concentration, $\dot{H}_{wet} = \dot{H}_{dry} + \dot{V}l_h\Delta C$, where ΔC is the difference in mass concentration of the water vapor, corresponding with the temperature difference. For example, a relative humidity of 80% $\Delta C = 0.008\,\mathrm{kg/m^3}$ is assumed, resulting in

$$\frac{\dot{H}_{wet}}{\dot{H}_{dry}} = 1 + \frac{l_h\Delta C}{\rho c_p \Delta T} \approx 4.5, \tag{6}$$

which illustrates that, in the wet case, the streaming heat flux under identical temperature difference and streaming velocity is much higher. The deviation between model and experiment in the wet case can likely be attributed to this effect. Additional explanations for the deviation can be the accumulation of water at some point in the resonator and variations in the value of ψ. We note that the assumption of a constant value for ψ is inaccurate, as the thermal contact varies during the acoustic cycle.[35]

Ultimately, the results are indicative of significant pressure amplification, due to the combined effect of input modulation and transport within a properly phased acoustic field. In particular, the results establish the effect of phase change on the enhancement of acoustic conversion, with a simplified model that provides reasonable corroboration. These findings can be considered as a first step toward designing a different type of thermoacoustic engine, based on alternating radiation—a resonator could be illuminated by periodic intermission of a light source, or by alternately turning the radiation source toward and away from the resonator. With improved efficiency, such devices can convert solar energy into sound waves, which in turn could be used for electricity generation, cooling, and other applications that require mechanical compression.

See the supplementary material for a picture of the experimental system, the full equations used in the model, raw numerical results compared to the experimental results, and a discussion on the effect of ambient conditions and air humidity on the results.

AUTHOR DECLARATIONS
Conflict of Interest

The authors have no conflicts to disclose.

Author Contributions

Nathan Blanc: Conceptualization (equal); Methodology (equal); Software (lead); Writing – original draft (equal); Writing – review & editing (equal). **Guy Z. Ramon:** Conceptualization (equal); Funding acquisition (equal); Methodology (supporting); Project administration (equal); Resources (equal); Writing – original draft (equal); Writing – review & editing (equal).

DATA AVAILABILITY

The data that support the findings of this study are available from the corresponding author upon reasonable request.

REFERENCES

[1]B. Chen, P. Riley, Y. Abakr, K. Pullen, D. Hann, and C. Johnson, "Design and development of a low-cost, electricity-generating cooking score-stove," Proc. Inst. Mech. Eng., Part A **227**, 803–813 (2013).

[2]X. Wang, J. Xu, Z. Wu, and E. Luo, "A thermoacoustic refrigerator with multiple-bypass expansion cooling configuration for natural gas liquefaction," Appl. Energy **313**, 118780 (2022).

[3]Z. Yang, Y. Zhuo, L. Ercang, and Z. Yuan, "Travelling-wave thermoacoustic high-temperature heat pump for industrial waste heat recovery," Energy **77**, 397–402 (2014).

[4]S. L. Garrett, "Reinventing the engine," Nature **399**, 303–305 (1999).

[5]Y. Chao, B. Wang, H. Li, M. Xia, Q. Zhao, H. Wang, R. Li, J. Chen, and Z. Gan, "A two-stage thermally-coupled pulse tube cryocooler working at 35 k for space application," Acta Astronaut. **191**, 193–203 (2022).

[6]G. Swift, *Thermoacoustics - A Unifying Perspective for Some Engines and Refrigerators* (Springer, 2002).

[7]A. G. Bell, "On the production and reproduction of sound by light" (1880).

[8]A. B. E. Attia, G. Balasundaram, M. Moothanchery, U. Dinish, R. Bi, V. Ntziachristos, and M. Olivo, "A review of clinical photoacoustic imaging: Current and future trends," Photoacoustics **16**, 100144 (2019).

[9]G. A. West, J. J. Barrett, D. R. Siebert, and K. V. Reddy, "Photoacoustic spectroscopy," Rev. Sci. Instrum. **54**, 797–817 (1983).

[10]R. Raspet, W. V. Slaton, W. P. Arnott, and H. Moosmüller, "Evaporation–condensation effects on resonant photoacoustics of volatile aerosols," J. Atmos. Oceanic Technol. **20**, 685–695 (2003).

[11]D. M. Murphy, "The effect of water evaporation on photoacoustic signals in transition and molecular flow," Aerosol Sci. Technol. **43**, 356–363 (2009).

[12]W. P. Arnott, H. Moosmüller, C. F. Rogers, T. Jin, and R. Bruch, "Photoacoustic spectrometer for measuring light absorption by aerosol: Instrument description," Atmos. Environ. **33**, 2845–2852 (1999).

[13]W. Slaton, R. Raspet, C. Hickey, and R. Hiller, "Theory of inert gas-condensing vapor thermoacoustics: Transport equations," J. Acoust. Soc. Am. **112**, 1423–1430 (2002).

[14]R. Raspet, W. V. Slaton, C. J. Hickey, and R. A. Hiller, "Theory of inert gas-condensing vapor thermoacoustics: Propagation equation," J. Acoust. Soc. Am. **112**, 1414–1422 (2002).

[15]K. Tsuda and Y. Ueda, "Abrupt reduction of the critical temperature difference of a thermoacoustic engine by adding water," AIP Adv. **5**, 097173 (2015).

[16]A. Meir, A. Offner, and G. Z. Ramon, "Low-temperature energy conversion using a phase-change acoustic heat engine," Appl. Energy **231**, 372–379 (2018).

[17]A. Offner, R. Yang, D. Felman, N. Elkayam, Y. Agnon, and G. Z. Ramon, "Acoustic oscillations driven by boundary mass exchange," J. Fluid Mech. **866**, 316–349 (2019).

[18]T. Brustin, A. Offner, and G. Z. Ramon, "Effect of gas mixture on temperature and mass streaming in a phase-change thermoacoustic engine," Appl. Phys. Lett. **116**, 243701 (2020).

[19]R. Yang, N. Blanc, and G. Z. Ramon, "Environmentally-sound: An acoustic-driven heat pump based on phase change," Energy Convers. Manage. **232**, 113848 (2021).

[20]R. Yang, A. Meir, and G. Ramon, "Theoretical performance characteristics of a travelling-wave phase-change thermoacoustic engine for low-grade heat recovery," Appl. Energy **261**, 114377 (2020).

[21]D. Gedeon, "A globally-implicit stirling cycle simulation," in *Intersociety Energy Conversion Engineering Conference* (U. S. Department of Energy, 1986), Vol. 21, pp. 550–554.

[22]L. Xiao, J. Xu, K. Luo, G. Chen, and E. Luo, "Numerical study of a heat-driven thermoacoustic refrigerator based on a time-domain lumped acoustic–electrical analogy model," Energy Convers. Manage. **268**, 115982 (2022).

[23]T. L. Bergman, T. L. Bergman, F. P. Incropera, D. P. Dewitt, and A. S. Lavine, *Fundamentals of Heat and Mass Transfer* (John Wiley & Sons, 2011).

[24]P. Cheng and T. Zhao, "Heat transfer in oscillatory flows," Annu. Rev. Heat Transfer **9**, 359–420 (1998).

[25]M. Ni, B. Shi, G. Xiao, Z. Luo, and K. Cen, "Heat transfer characteristics of the oscillating flows of different working gases in u-shaped tubes of a stirling engine," Appl. Therm. Eng. **89**, 569–577 (2015).

[26]A. Piccolo and G. Pistone, "Estimation of heat transfer coefficients in oscillating flows: The thermoacoustic case," Int. J. Heat Mass Transfer **49**, 1631–1642 (2006).

[27]"Prediction of oscillatory heat transfer coefficient in heat exchangers of thermo-acoustic systems," in ASME International Mechanical Engineering Congress and Exposition, Vol. Volume 8: Heat Transfer and Thermal Engineering (2019).

[28]G. W. Swift, "Thermoacoustic engines," J. Acoust. Soc. Am. **84**, 1145–1180 (1988).

[29]D. H. Keefe, "Physical modeling of wind instruments," Comput. Music J. **16**, 57–73 (1992).

[30]G. W. Swift, "Analysis and performance of a large thermoacoustic engine," J. Acoust. Soc. Am. **92**, 1551–1563 (1992).

[31]G. Y. Yu, E. C. Luo, W. Dai, and J. Y. Hu, "Study of nonlinear processes of a large experimental thermoacoustic-Stirling heat engine by using computational fluid dynamics," J. Appl. Phys. **102**, 074901 (2007).

[32]O. Weltsch, A. Offner, D. Liberzon, and G. Z. Ramon, "Adsorption-mediated mass streaming in a standing acoustic wave," Phys. Rev. Lett. **118**, 244301 (2017).

[33]U. Ingård and S. Labate, "Acoustic circulation effects and the nonlinear impedance of orifices," J. Acoust. Soc. Am. **22**, 211–218 (1950).

[34]C. Eckart, "Vortices and streams caused by sound waves," Phys. Rev. **73**, 68 (1948).

[35]M. Azadi, A. Jafarian, and M. Timaji, "Analytical investigation of oscillating flow heat transfer in pulse tubes," Sci. Iran. **20**, 483–491 (2013).

25 October 2023 12:52:10